

Estimation of speed in linear induction motor drive by MRAS using neural network and sliding mode control

M. Anka Rao¹, M. Vijaya kumar², O. Yugeswar Reddy³

¹ Asst. Professor, Dept. of Electrical Engg., JNTUA College of Engineering, Anantapuramu, India-515002

² Professor, Dept. of Electrical Engg., JNTUA College of Engineering, Anantapuramu, India - 515002

³ M.Tech Student, Dept. of Electrical Engg., JNTUA College of Engineering, Anantapuramu, India - 515002

Abstract: The paper proposes a speed observer for a linear induction motor drive, which uses artificial neural network model reference adaptive system (NN-MRAS) that uses sliding mode control. The basic mathematical equations of the motor governed by the voltages and currents from the equivalent circuit of the motor including the end effects are determined. The artificial neural network (ANN) model based adaptive system in MRAS for the secondary of the motor is developed. The sliding mode control is implemented with the NN-MRAS model. The dynamical response and speed observation is compared for the conventional MRAS using PI control and the NN-MRAS with sliding mode control model for the induction motor drive by simulation using Matlab/Simulink.

KEY WORDS: Indirect vector control, linear induction motor, MRAS, artificial neural network, sliding mode control.

I. Introduction

Every strategy or methodology that needs to be studied and implemented initiates with the motor drive that is dealt with. The induction motor drives have a recent and fast development in various applications due to its gaining edge compared to the dc motor drives. Linear induction motors are a special type of induction motor that have been studied and for linear motion applications [2]. Unlike rotator induction motors (RIM), linear induction motors (LIM) do not require motion conversion from rotator to linear form. Many recent literatures related to LIM are present. Even though LIM have their advantages, there are some difficulties in analysing and modelling it due to complexity of structure. End effects are associated with the machine due to asymmetric structure. Linear encoders are used for the speed control of the motor which is costly and have low reliability. So, sensors less techniques are used for reducing the difficulty [3], [4], [7], [8]. But accurate measurement in speed of ac motor is still not possible [5], [6]. The conventional MRAS has been implemented on RIM. The NN MRAS has been tested on RIM and LIM with PI controller [11], [1], [9], [10]. The model is deduced from basic voltage and current models of LIM. MRAS that uses ANN in the adaptive model is developed based on the

equations of the motor [1]. The sliding mode control replaces the conventional PI control and simulated. The NN-MRAS model and the conventional model are compared for the performance.

II. Equivalent circuit of LIM

The primary difference between the transformer and induction motor is related to effects of varying rotor frequency on rotor voltages and impedances. The linear induction motor generalised model and equivalent circuit is shown in the figure.

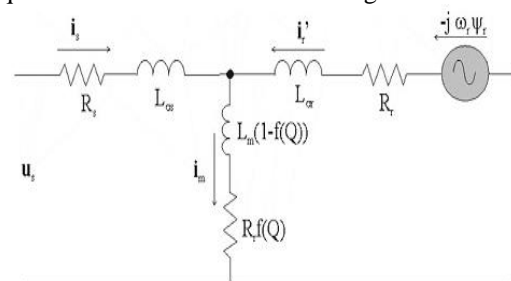


Fig. 1. Equivalent circuit of LIM

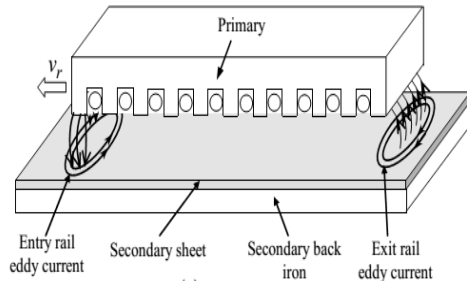


Fig.2. Generalised model of LIM

The primary is basically stationary, similar to RIM but cut opened and rolled flat. The currents produce magnetic field translational to the surface of the stator. The secondary is a piece of conductor with iron return path i.e. for the magnetic flux to pass. There are basically two types of construction single sided and double sided.

III. Mathematical model

The mathematical model [12] is derived from basic induced voltage equations of an induction motor except this includes the end effects in the model. The end effects are occurred during the motion between the stator (primary) and secondary. The difference in the induced currents causes the difference in the magnetic flux density at both the ends. The end effects behave differently at the entry and exit ends of the LIM. The currents induced in the secondary at the entry end decay more slowly than at the exit end, because of its larger time constant. It depends on the velocity of the secondary. The primary's length is inversely proportional to the velocity, i.e., for a zero velocity the primary's length may be considered infinite, and the end effects may be neglected. The effect is governed by the equation, $f(Q) = (1 - e^{-Q})/Q$; and Q is given as $Q = DR_r / (L_m + L_{lr})v$, where D is length, L_{lr} is secondary leakage reactance, L_m is mutual inductance, R_r is the secondary resistance and v is the velocity of secondary.

$$V_{ds} = R_s i_{ds} + R_r f(Q) (i_{ds} + i_{dr}) + p\lambda_{ds} - \omega_e \lambda_{qs} \quad (1)$$

$$V_{qs} = R_s i_{qs} + p\lambda_{qs} - \omega_e \lambda_{ds} \quad (2)$$

$$V_{dr} = R_r i_{dr} + R_r f(Q) (i_{ds} + i_{dr}) + p\lambda_{dr} - \omega_{sl} \lambda_{qr} \quad (3)$$

$$V_{qr} = R_r i_{qr} + p\lambda_{qr} - \omega_{sl} \lambda_{dr} \quad (4)$$

$$\lambda_{ds} = L_{ls} i_{ds} + L_m (1 - f(Q)) (i_{ds} + i_{dr}) \quad (5)$$

$$\lambda_{qs} = L_{ls} i_{qs} + L_m (i_{qs} + i_{qr}) \quad (6)$$

$$\lambda_{dr} = L_{lr} i_{dr} + L_m (1 - f(Q)) (i_{ds} + i_{dr}) \quad (7)$$

$$\lambda_{qr} = L_{lr} i_{qr} + L_m (i_{qr} + i_{qs}) \quad (8)$$

The flux equations can be split into two parts while modeling. The first part consists of the equation without the end effect and the second equation includes the end effects.

IV. Indirect vector oriented control for LIM

Basically there are two types of vector control, direct and indirect. The sensor less techniques that are used generally uses the latter type of control of speed [13]-[15]. The three phase flux is transformed into dq-axes which are orthogonal and the secondary currents are decoupled in the direct and quadrature axes. Here, vector oriented control is used for the secondary induced flux of the LIM. The block diagram showing the vector control is shown in the figure. The current control is done in secondary oriented reference frame. The direct and quadrature axes are controlled by a flux control loop and a speed loop respectively. The angular position that is required for the estimation of speed is provided by the NN-MRAS with sliding mode control. The conventional MRAS uses PI controllers. The pulse width modulation which uses space vector modulation is used for the motor input. The transformations from the 3-phase to dq and back are also shown in the block diagram. There exist some minor problems related to the implementation. Due to the presence of dc biases, there exists open loop integration causing integrator to saturate. There is also the inverter nonlinearity due to the presence of finite voltage drop during its on-state.

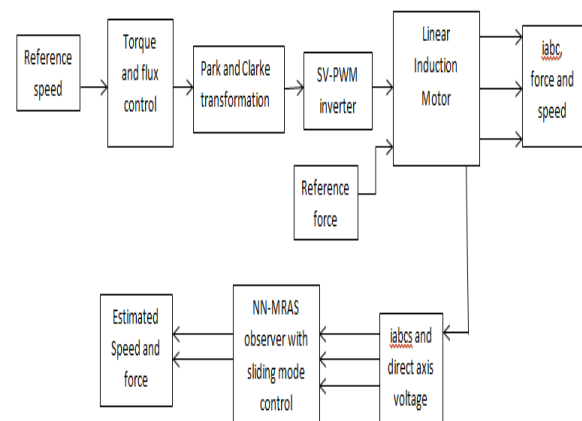


Fig.3. Block diagram for vector control of LIM

V. MRAS using neural network and sliding mode control

In the model reference adaptive system (MRAS) technique [16], the reference model output is compared to an adjustable/adaptive model output until the error is minimized. Since it cannot become practically zero tolerance limits can be set. The reference model is modeled on primary equations

and the adaptive model is modeled on the secondary equations. The equations that are governing the reference and adaptive model derived from the equivalent circuit are:

$$d\Psi_r'/dt = u_s - R_s i_s - L_s di_s/dt - R_r f(Q) \Psi_r' / L_m (1 - f(Q)) \quad (9)$$

$$d\Psi_r'/dt = R_r i_s + (j p \pi v / \tau_p - R_r (1 + f(Q)) / L_m (1 - f(Q))) \Psi_r' \quad (10)$$

These are the voltage and current models respectively. The equations are derived in the secondary oriented reference frame of the secondary induced flux. The linear speed is estimated from the rotating speed by the equation $\omega_r = (D\pi/\tau_p)v$ and the force is derived from the torque equation as

$F_e = 3\pi P (\lambda_{ds} i_{qs} - \lambda_{qs} i_{ds}) / 4\tau_p$. In the MRAS, the reference model is modeled based on (9) and the adaptive model is modeled based on (10). For the adaptive model, an artificial neural network is developed using (10), where the NN model is a linear neural network called ADALINE model. The block diagram of the MRAS system is shown in the figure.

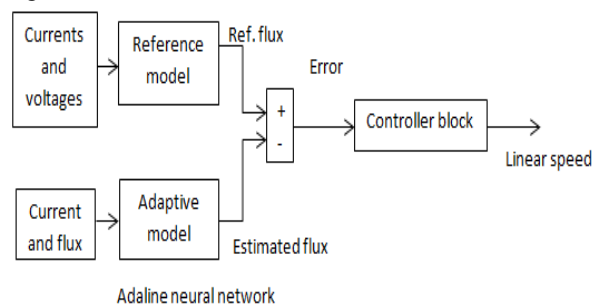


Fig.4. MRAS block diagram using NN

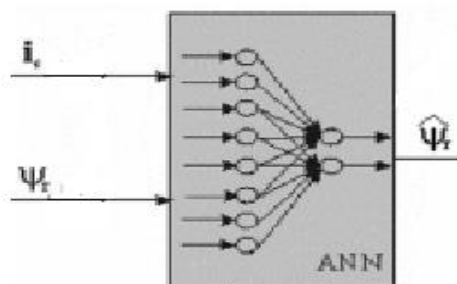


Fig.5. Neural network model

The neural network used is a simple adaline model as shown in the figure. The model uses two inputs and one output with single layer neurons. The two inputs are currents and flux from the feedback. The flux output is the estimated which on compared with the reference flux gives the speed estimated.

The error is minimized by the controller, here sliding mode control. On using a sliding mode controller, the effective gains of the error compensator can be increased to adjust the observer for both speed adaptation and for secondary flux estimation. The performance provided is robust with variations parameter changes and torque changes that are caused due to load variations, etc. A switch algorithm is used for the control and so it behaves as a nonlinear control. Here, the conventional and general controllers used i.e. PI are replaced by the sliding mode controller. The conventional MRAS model using PI controller and the proposed NN-MRAS model using sliding mode controller are compared in the dynamic performance criteria for the motor drive and results are shown.

VI. Simulation Results

The linear induction motor model has been modelled using the equations and simulated in Matlab/Simulink. The neural network based MRAS system with sliding mode controller is simulated along with the conventional MRAS model and the results of the models in Matlab/Simulink are compared. The parameters of the motor drive are shown in the table.

Table 1
Parameters of LIM

Rated voltage [V]	400
Rated frequency [Hz]	50
Pole pairs	6
Stationary resistance $R_s[\Omega]$	0.855
Stationary inductance $L_s[mH]$	0.100792
Secondary resistance $R_r[\Omega]$	1.15
Secondary inductance $L_r[mH]$	0.100792
Magnetizing inductance $L_m[mH]$	0.1004
Inertia J	0.06

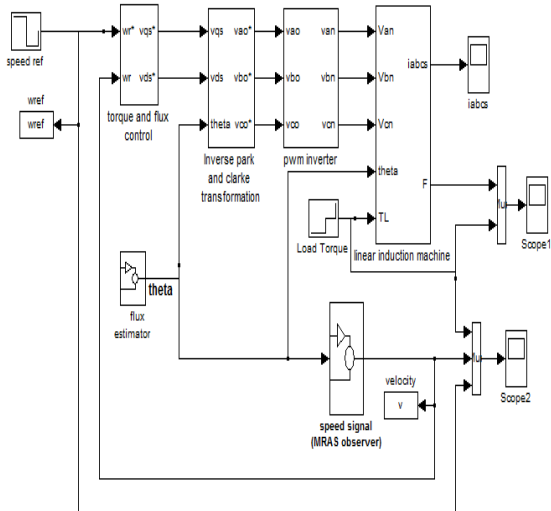


Fig.6. Simulation model of speed estimation using NN-MRAS and sliding mode control for LIM drive

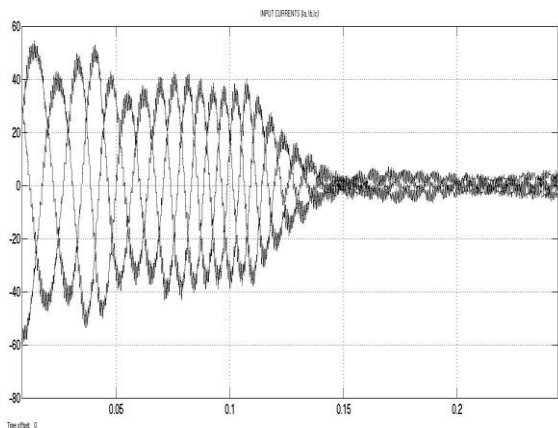


Fig.7. I_{abc} currents of conventional MRAS model

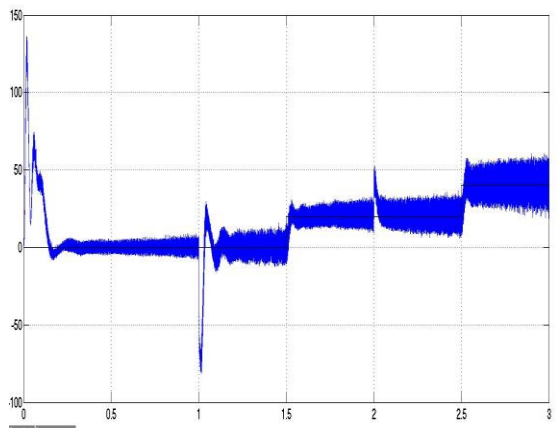


Fig.8. Reference and estimated torque of conventional MRAS model

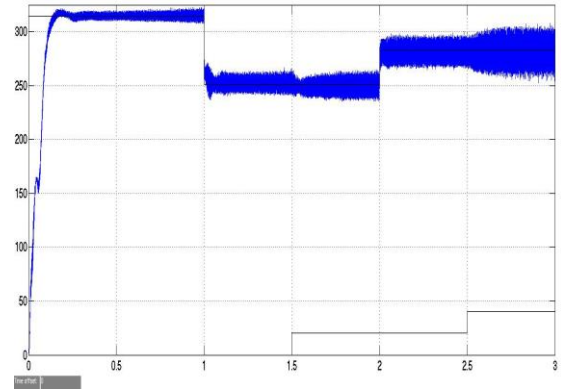


Fig.9. Reference and estimated speed of conventional MRAS model

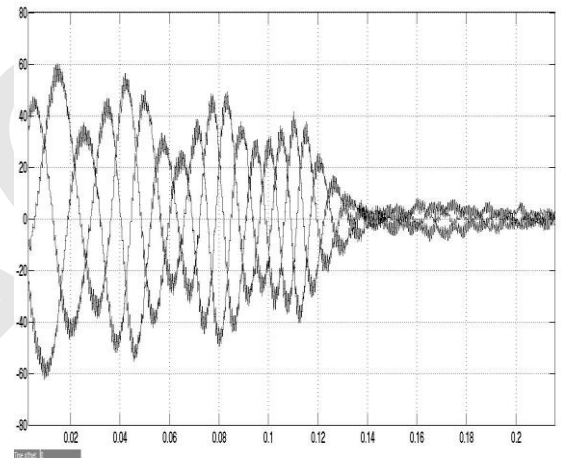


Fig.10. I_{abc} currents of NN-NRAS model

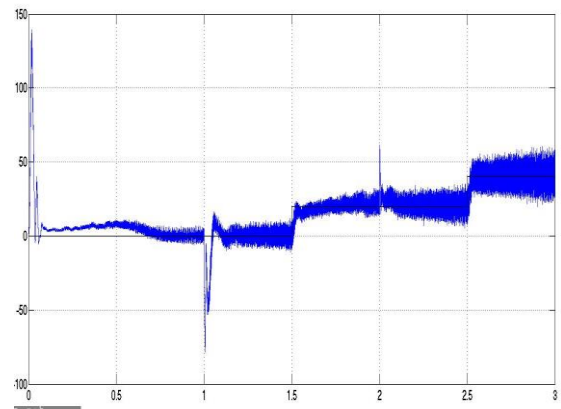


Fig.11. Reference and estimated torque of NN-NRAS model

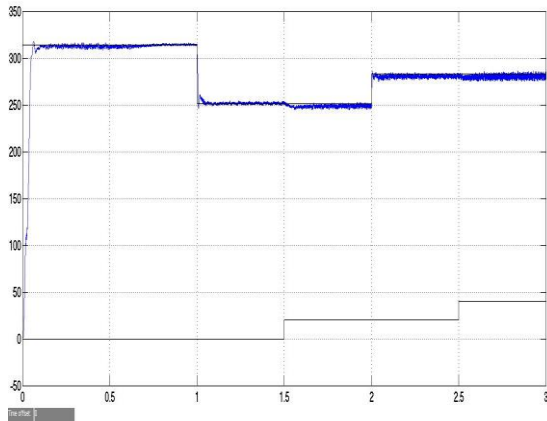


Fig.12. Reference and estimated speed of NN-NRAS model

The figures 7 and 10 show the primary currents. The figures 8 and 11 show the variation in load torque in steps from 0 to 45N-m. The figures 9 and 12 show the speed response when it is estimated and the error tracking comparison which is improved as expected. The speed is also varied in steps from 320 to 250 and 250 to 280. The dynamic performance has been compared with respect to torque (output generally is force) and speed of the secondary with varying loads or here step changes are considered. The speed is varied in the positive values which we can consider it as the secondary moves in one direction. The reverse direction of the same can also be analyzed by comparing and we get similar results. The plots are shown for the primary currents and time, torque and time and speed and time. As expected, from the two plots we can observe that the estimated speed, torque tracks their respective references reducing the error. The harmonics are present in the system when the drive is modeled which can be observed in the plots. These represent the imperfect decoupling of the orthogonal axes components of flux. The harmonics in the primary currents are also reduced by using the NN-NRAS model.

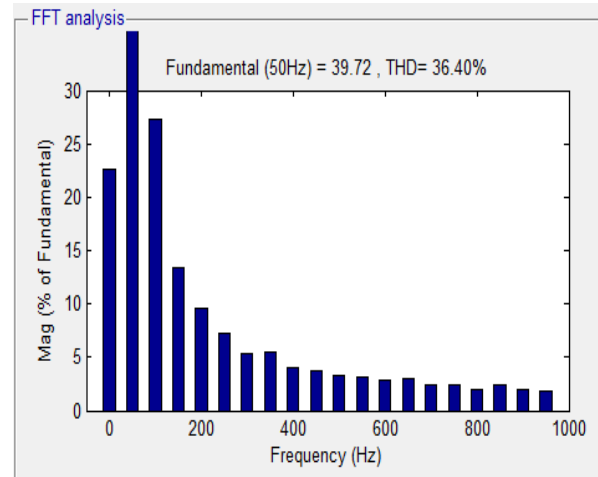


Fig.13. THD of conventional MRAS model

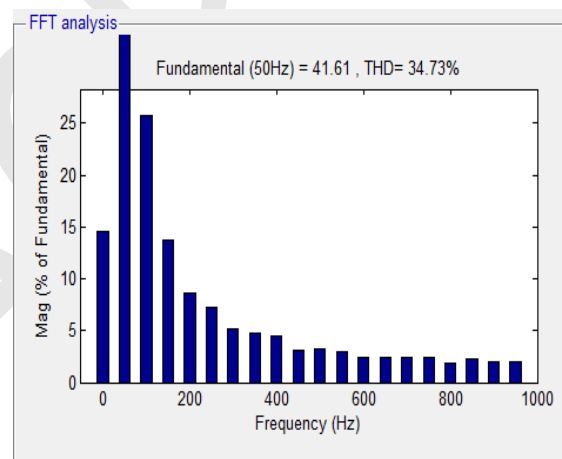


Fig.14. THD of NN-MRAS model

VII. Conclusion

This paper finally proposes an artificial neural network based MRAS system by sliding mode control for speed estimation of a linear induction motor drive. Initially, from the equivalent circuit, the expressions are derived and modeled for LIM. Then a NN adaptive system for MRAS is developed based on the secondary induced equations. The sliding mode controller replaces the conventional PI controller. The THD is also improved in the proposed NN-MRAS model shown in the figures 13 and 14. The table shows the steady state responses and comparison of both the models.

Table 2

Comparison of results between conventional MRAS and proposed NN-MRAS model

	MRAS with PI control	NN-MRAS with sliding mode

			control
Torque(N-m)	Rise Time	0.0052	0.0047
	Settling Time	3.0000	2.5724
	Settling Min	-135.0082	-81.3612
	Settling Max	154.5103	135.8739
	Overshoot	239.4137	155.6759
	Undershoot	296.5731	153.0985
	Peak	154.5103	135.8739
	Peak Time	0.0194	0.0175
Speed(rpm)	Rise Time	0.0842	0.0827
	Settling Time	2.9999	2.0001
	Settling Min	235.5970	245.2452
	Settling Max	322.9322	318.8419
	Overshoot	12.9017	8.0371
	Undershoot	1.2755e-004	5.9037e-004
	Peak	322.9322	318.8419
	Peak Time	0.9847	0.1867
THD		36.40%	34.73%

The conventional MRAS model is also modeled. Both the models are simulated in Matlab/Simulink. The results display that the dynamic performance of the proposed NN-MRAS model is better than the conventional MRAS model and also the harmonics are reduced in the proposed NN-MRAS model.

References

- [1] Maurizio Cirrincione, Angelo Accetta, Marcello Pucci and Gianpaolo Vitale, "MRAS Speed Observer for High-Performance Linear Induction Motor Drives Based on Linear Neural Networks", IEEE Trans. on Power Electronics, vol. 28, no. 1, January 2013.
- [2] E. R. Laithwaite, "Linear electric machines—A personal view," Proc. IEEE, vol. 63, no. 2, pp. 250–290, Feb. 1975.
- [3] K. Rajashekara, A. Kawamura, and K. Matsuse, Sensorless Control of AC Motor Drives. New York: IEEE Press, 1996.
- [4] J. Holtz, "Sensorless control of induction motor drives," Proc. IEEE, vol. 90, no. 8, pp. 1359–1394, Aug. 2002.
- [5] Y. Zhang, J. Zhu, Z. Zhao, W. Xu, and D. G. Dorrell, "An improved direct torque control for three-level inverter-fed induction motor sensorless drive," IEEE Trans. Power Electron., vol. 27, no. 3, pp. 1502–1513, Mar. 2012.
- [6] L. de Henriques, L. Rolim, W. Suemitsu, J. A. Dente, and P. J. Branco, "Development and experimental tests of a simple neurofuzzy learning sensorless approach for switched reluctance motors," IEEE Trans. Power Electron., vol. 26, no. 11, pp. 3330–3344, Nov. 2011.
- [7] C.-I. Huang, F. Li-Chen, W.-Y. Jywe, and J. C. Shen, "Speed motionsensorless with adaptive control approach of linear induction motor unknown resistance and payload", in IEEE Power Electron. Spec. Conf., Jun. 15–19, 2008, pp. 3887–3893.
- [8] H.-M. Ryu, J.-I. Ha, and S.-K. Sul, "A new sensorless control thrust control of linear induction motor," in Proc. IEEE Ind. Appl. Conf., 2000, vol. 3, pp. 1655–1661.
- [9] M. Pucci, A. Sferlazza, G. Vitale, and F. Alonge, "MRAS sensorless techniques for high performance linear induction motor drives," presented at the IEEE Int. Power Electron. Motion Control Conf., Ohrid, Macedonia, Sep. 6–8, 2010.
- [10] M. Cirrincione, M. Pucci, A. Sferlazza, and G. Vitale, "Neural based MRAS sensorless techniques for high performance linear induction motor drives," in Proc. 36th Annu. Conf. Ind. Electron. Soc., Nov. 7–10, Phoenix, AZ, pp. 918–926.
- [11] C. Shauder, "Adaptive speed identification for vector control of induction motors without rotational transducers," IEEE Trans. Ind. Appl., vol. 28, no. 5, pp. 1054–1061, Sep./Oct. 1992.
- [12] J. Duncan, "Linear induction motor-equivalent- circuit model," IEE Proc.-Electr. Power Appl., vol. 130, no. 1, pp. 51–57, 1983.
- [13] J. H. Sung and K. Nam, "A new approach to vector control for a linear induction motor considering end effects," in Proc. IEEE 34th IAS Annu. Meet. Ind. Appl. Conf., 1999, vol. 4, pp. 2284–2289.
- [14] G. Kang and K. Nam, "Field-oriented control scheme for linear induction motor with the end effect," IEE Proc.-Electr. Power Appl., vol. 152, no. 6, pp. 1565–1572, Nov. 2005.
- [15] V. Isastia, G. Gentile, S. Meo, A. Ometto, N. Rotondale, and M. Scarano, "A voltage feeding algorithm for vectorial control of linear asynchronous machines taking into account end effect," in Proc. Int. Conf. Power Electron. Drives Energy Syst. Ind. Growth, 1998, vol. 2, pp. 729–734.